Existence domains of electrostatic solitary structures in the solar wind plasma

R. Rubia,[1,a)] S. V. Singh,[1,2,b)] and G. S. Lakhina[1,2,c)]

[1]*Indian Institute of Geomagnetism, Navi Mumbai, India*
[2]*University of the Western Cape, Bellville 7535, Cape Town, South Africa*

Electrostatic solitary waves and double layers are explored in a homogeneous, collisionless, and magnetized three-component plasma composed of hot protons, hot heavier ions (alpha particles, He^{++}), and suprathermal electrons with kappa distribution. The Sagdeev pseudopotential technique is used to study the arbitrary amplitude ion-acoustic solitons and double layers. The effect of various parameters such as the number density of ions, n_{i0}; the spectral index, κ; the Mach numbers, M; and the temperature ratio of ion to the electron σ_i on the evolution of ion-acoustic solitary waves as well as their existence domains is studied. The transition in the existence domain for slow-ion acoustic solitons from negative solitons/double layers to positive solitons/double layers is found to occur with a variation of the heavier ion temperature. It is observed that the width of the negative potential solitons increases as the amplitude increases, whereas for the positive potential solitons, the width decreases as the amplitude increases. Furthermore, it is found that the limitation on the attainable amplitudes of fast ion-acoustic solitons is attributed to that the number density of protons should remain real valued, while for the slow ion-acoustic solitons, the upper limit is provided by the requirement that the number density of heavier ions should remain real. In the presence of a double layer, the occurrence of the double layer limits the attainable amplitudes of the slow ion-acoustic solitons. The proposed plasma model is relevant to the coherent electrostatic structures observed in the solar wind at 1 AU. *Published by AIP Publishing.*
[http://dx.doi.org/10.1063/1.4953892]

I. INTRODUCTION

Electrostatic solitary waves in multi-species plasmas have been studied extensively for over several decades. Washimi and Taniuti[1] analyzed the propagation of ion-acoustic solitons in a two component plasma consisting of cold ions and warm electrons using finite, small amplitude theory. Theoretical as well as experimental investigations on the propagation of ion-acoustic solitons in a two electron temperature plasma were carried out by Jones *et al.*[2] Ion acoustic waves were analyzed in a plasma with hot and cold electron by Goswami and Buti.[3] It was found that when the temperature difference between the two electron components was sufficiently large, solitary solution ceased to exist. Baboolal *et al.*[4] investigated the existence domains of ion-acoustic solitons and double layers (DLs) for two Boltzmann electron components and single cool ion. Cairns *et al.*[5] investigated the oblique propagation of ion-acoustic solitons in a two component magnetized plasma with non-thermal electrons. Berthomier *et al.*[6] utilized two-electron temperature auroral plasma model to explain the observed ion-acoustic solitary structures and weak double layers by Viking Satellite.

Ghosh and Lakhina[7] studied the parallel and oblique propagation of ion-acoustic solitons in a two electron temperature multi-ion-plasma. They were able to explain the POLAR satellite observations of the solitary structures in the auroral region. Singh *et al.*[8] studied arbitrary amplitude electron-acoustic solitons and double layers in an unmagnetized four component plasma consisting of non-thermally distributed hot electrons, fluid cold electrons, and warm electron beam and ions. They found that the existence of positive potential solitons is determined by the warm electron component having intermediate temperature between hot and cold electron component rather than the beam speed. They also studied the existence domains for positive and negative polarity electrostatic solitons and double layers. They observed a transition from negative potential solitons/double layers to positive potential solitons/double layers as the number density of cool electrons is increased.

Ion and electron acoustic solitons in an unmagnetized plasma with cold and hot electrons and hot ions were analyzed by Lakhina *et al.*[9] They found that the electron-acoustic solitons have larger critical Mach number as compared to ion-acoustic solitons for a given set of plasma parameters. They were able to explain the solitary waves observed in the auroral field lines by the Viking spacecraft. Lakhina *et al.*[10] extended the analysis by including hot ion beam in the system. Furthermore, they considered the hot electrons in the system to have a beam component. It was observed that in addition to the electron acoustic solitons, slow and fast ion-acoustic solitons also existed. The slow ion acoustic solitons were found above the lowest critical Mach number.

Maharaj *et al.*[11] analyzed the existence domains of arbitrary amplitude solitons in a three component plasma composed of ions, and hot and cool electrons. They found that

---

a)Electronic mail: rubi.r92@gmail.com
b)Electronic mail: satyavir@iigs.iigm.res.in
c)Electronic mail: gslakhina@gmail.com

when the temperature of cool electrons is negligible, small amplitude solitons with negative potentials existed. They studied the existence domains of ion-acoustic solitons as a function of cool electron number density and hot electron temperature. They found that the model supported only positive potential ion-acoustic solitons when the cool electron has finite but small pressure. Furthermore, it was found that the upper limit on the Mach number for the solitons was imposed by the number density of ions having to be real valued. Existence domains of both slow and fast ion-acoustic solitons in a four component plasma comprised of both hot and cold electrons and ions were investigated by Maharaj et al.[12] The fast ion-acoustic solitons were found to have only positive potentials, while slow ion-acoustic mode supports both positive potential solitons/double layers and negative potential solitons/double layers. They reported a transition from a positive potential double layer to a negative potential double layer as cool ion number density increases.

Electrostatic waves with frequencies between ion and electron plasma frequencies were observed in the solar wind by Gurnett and Anderson.[13] On the basis of the wavelength measurement by the Imp6 spacecraft, Gurnett and Frank[14] reported the presence of ion-acoustic waves in the solar wind. Mangeney et al.[15] discussed the new observations made by the WIND spacecraft. Their analysis of the high-time resolution electric field data collected by the Time Domain Sampler (TDS) instrument onboard the Wind spacecraft showed the presence of coherent electrostatic waves in the ion-acoustic frequency range, falling between the ion and electron plasma frequencies, in the solar wind at 1 AU. They also found Langmuir waves and isolated electrostatic structures (IES) along with ion-acoustic waves. For the first time, they reported the observed IES, which can be explained in terms of weak double layers. Malaspina et al.[16] observed the electric bipolar structures of solitary waves in the electric field data obtained from the WIND.

Lakhina et al.[17] investigated the ion acoustic solitons and double layers in a three component plasma consisting of cold heavier ions, warm lighter ions, and hot electrons having Boltzmann distribution. On inclusion of thermal effects of the lighter ion species, they found that in addition to the usual fast ion-acoustic solitons, a new slow ion-acoustic mode appears, which supported both positive and negative potential solitons/double layers. Lakhina and Singh[18] extended their model to include hot heavier ions streaming with finite drift velocity with respect to the lighter ions, and electrons having kappa distribution. They applied it to explain the low frequency electrostatic waves observed in the solar wind at 1 AU by WIND.

In this paper, we study the ion-acoustic solitons and double layers observed in the solar wind plasma by Sagdeev pseudopotential technique. Our model consists of hot protons, hot alpha particles, and kappa-distributed suprathermal electrons. Here, the "hot" signifies that the temperature of both the protons and alpha particles is finite. The existence domains of slow and fast ion-acoustic solitons are examined as a function of the number density of the heavier ions, spectral index, κ, and temperature of heavier ions. In the past, polarity switches of the various electrostatic solitons and

double layers have been examined in terms of density of one of the ion/electron species in multi-component plasmas. Here, for the first time, we report a transition from negative to positive polarities of solitons and double layers with respect to the temperature variation of the heavier ions.

The outline of the paper is as follows. In Sec. II, a theoretical model is presented, and the results are discussed in Sec. III. The conclusions of our observations are presented in Sec. IV.

II. THEORETICAL MODEL

We consider a homogeneous, collisionless, and magnetized three-component plasma comprising of protons (N_{p0}, T_p), heavier ions, i.e., alpha particles, He^{++} (N_{i0}, T_i), and suprathermal electrons (N_{e0}, T_e) to model the solar wind plasma. Here, N_{j0} and T_j represent the equilibrium values of the density and temperature of the species j, and j = p, i, and e for protons, heavier ions, and suprathermal electrons, respectively. The electrostatic solitary waves are assumed to be propagating parallel to the ambient magnetic field.

The suprathermal electrons are assumed to follow the κ (Kappa)-distribution given by[19]

$$f_e(\nu) = \frac{N_{e0}}{\pi^{3/2}\theta^3}\frac{\Gamma(\kappa)}{\sqrt{\kappa}\,\Gamma(\kappa - 1/2)}\left(1 + \frac{\nu^2}{\kappa\theta^2}\right)^{-(\kappa+1)}, \quad (1)$$

where κ is the spectral index with $\kappa > 3/2$, $\Gamma(\kappa)$ is the gamma function, and θ is the modified electron thermal speed given by

$$\theta^2 = \left(2 - \frac{3}{\kappa}\right)\frac{T_e}{m_e}.$$

Here, T_e and m_e are the electron temperature and the electron mass, respectively. When $\kappa \to \infty$, the kappa-distribution approaches a Maxwellian distribution.

As described by Lakhina and Singh,[18] the number density of electrons in the presence of ion-acoustic waves is obtained as[20]

$$n_e = \left(1 - \frac{\phi}{\kappa - 3/2}\right)^{-\kappa+1/2}. \quad (2)$$

In Eq. (2), the electron number density and the electrostatic potential have been normalized by N_{e0} and T_e/e, respectively.

The governing normalized fluid equations for parallel propagating ion acoustic solitons in the solar wind plasma are given by
the continuity equation

$$\frac{\partial n_j}{\partial t} + \frac{\partial (n_j v_j)}{\partial x} = 0, \quad (3)$$

the momentum equation

$$\frac{\partial v_j}{\partial t} + v_j\frac{\partial v_j}{\partial x} + Z_j\mu_{pi}\frac{\partial \phi}{\partial x} + 3\mu_{pi}\sigma_j\frac{n_j}{(n_{j0})^2}\frac{\partial n_j}{\partial x} = 0. \quad (4)$$

Poisson's equation

$$\frac{\partial^2 \phi}{\partial \xi^2} = (n_e - n_p - Z_i n_i). \quad (5)$$

In the Eq. (4), the momentum equation and the equation of state are combined together.

The normalizations used in Equations (2)–(5) are as follows: velocities are normalized with the ion-acoustic speed defined by electron temperature and proton mass $C_a = \sqrt{T_e/m_p}$, lengths with the effective hot electron Debye length $\lambda_{de} = \sqrt{T_e/4\pi N_0 e^2}$, and time with the inverse of the proton plasma frequency $\omega_{pp} = \sqrt{4\pi N_0 e^2/m_p}$. Here, $\mu_{pi} = m_p/m_i$, where m_p is the mass of proton and m_i is the mass of heavier ion. $\sigma_j = T_j/T_e$, where j = p and i, and $n_{j0} = N_{j0}/N_0$ is the equilibrium number density of jth species and $N_0 = N_{e0} = N_{p0} + Z_i N_{i0}$. v_j is the normalized fluid velocity. $Z_j = -1$ for electrons, $Z_j = +1$ for protons, and $Z_j = 2$ for heavier ions (alpha particles). Furthermore, we have taken the adiabatic index as $\gamma_j = 3$. This is justified for a one-dimensional case considered here.

In order to study the properties of arbitrary amplitude ion-acoustic solitary waves, we transform the above set of equations to a stationary frame moving with velocity V, the phase velocity of the wave, i.e., $\xi = x - Mt$, where $M = V/C_a$ represents the Mach number. In such a reference frame, as $\xi \to \pm\infty$, all variables, e.g., densities and pressure tend to their equilibrium values and potential, $\phi \to 0$. From, the Eqs. (3) and (4), we get the expressions for the density of protons, n_p, and heavier ions, n_i, which are similar to those equations reported by Lakhina and Singh[18] with $U_0 = 0$. Here, U_0 is the normalized relative drift between the protons and the heavier ion.

Multiplying Eq. (5) by $d\phi/d\xi$ and integrating it by using the appropriate boundary conditions gives the energy integral as

$$\frac{1}{2}\left(\frac{d\phi}{d\xi}\right)^2 + S(\phi, M) = 0, \quad (6)$$

where the Sagdeev pseudopotential, $S(\phi, M)$, is given by

$$S(\phi, M) = \frac{n_{p0}}{6\sqrt{3\sigma_p}}\left[\left(M + \sqrt{3\sigma_p}\right)^3 - \left\{\left(M + \sqrt{3\sigma_p}\right)^2 - 2\phi\right\}^{3/2} - \left(M - \sqrt{3\sigma_p}\right)^3 + \left\{\left(M - \sqrt{3\sigma_p}\right)^2 - 2\phi\right\}^{3/2}\right]$$

$$+ \frac{n_{i0}}{6\sqrt{3\sigma_i}}\left\{\left(\frac{M}{\sqrt{\mu_{pi}}} + \sqrt{3\sigma_i}\right)^3 - \left[\left(\frac{M}{\sqrt{\mu_{pi}}} + \sqrt{3\sigma_i}\right)^2 - 2Z_i\phi\right]^{3/2} - \left(\frac{M}{\sqrt{\mu_{pi}}} - \sqrt{3\sigma_i}\right)^3 + \left[\left(\frac{M}{\sqrt{\mu_{pi}}} - \sqrt{3\sigma_i}\right)^2 - 2Z_i\phi\right]^{3/2}\right\}$$

$$+ \left[1 - \left(1 - \frac{\phi}{\kappa - 3/2}\right)^{-\kappa + 3/2}\right]. \quad (7)$$

Equation (7) has been written in a symbolic form where the operation of a square root on a squared expression returns the same expression, e.g., $\sqrt{(M \pm \sigma_j)^2} = M \pm \sigma_j$.

For soliton solutions to exist, the Sagdeev pseudopotential $S(\phi, M)$ must satisfy the following conditions: (i) $S(\phi, M) = 0$, $dS(\phi, M)/d\phi = 0$, and $d^2S(\phi, M)/d\phi^2 < 0$ at $\phi = 0$, (ii) $S(\phi, M) = 0$ at $\phi = \phi_{max}$ (ϕ_{max} is the maximum amplitude), and (iii) $S(\phi, M) < 0$ for $0 < |\phi| < |\phi_{max}|$. Thus, when the conditions (i)–(iii) are satisfied, the pseudoparticle is reflected in the pseudopotential field and returns to its initial state (zero potential drop) for the solitary wave solution. Therefore, these are necessary conditions for the existence of the soliton solutions. Further, in addition to the soliton conditions (i)–(iii), the following condition should be satisfied for a double layer solution, (iv) $dS(\phi, M)/d\phi = 0$ at $\phi = \phi_{max}$. When the above additional condition (iv) is also satisfied, the pseudoparticle is not reflected at $\phi = \phi_{max}$ because of the vanishing pseudoforce and pseudovelocities. Instead, it goes to another state producing an asymmetrical double layer (DL) with a net potential drop of ϕ_{max}, where ϕ_{max} is the amplitude of a double layer. The applicability of these conditions can be verified from Figure 2(a) where Sagdeev potential is plotted for both solitons and a double layer. In the figure, the curve corresponding to a double layer is marked as DL.

From Eq. (7), it can be seen that the Sagdeev pseudopotential, $S(\phi, M)$, and its first derivative with respect to ϕ vanish at $\phi = 0$. Furthermore, the soliton condition $d^2S(\phi, M)/d\phi^2 < 0$ at $\phi = 0$ demands that $M > M_0$, where the critical Mach number, M_0, satisfies the following equation:

$$\frac{n_{p0}}{M^2 - 3\sigma_p} + \frac{n_{i0}Z_i^2}{\dfrac{M^2}{\mu_{pi}} - 3\sigma_i} - \left(\frac{\kappa - 1/2}{\kappa - 3/2}\right) = 0. \quad (8)$$

For the case of $n_{i0} = 0$, i.e., a two component plasma comprising of proton-electron, Eq. (8) has a single positive root, namely,

$$M_0 = \sqrt{\frac{\kappa - 3/2}{\kappa - 1/2} + 3\sigma_p}, \quad (9)$$

describing the ion-acoustic mode in a plasma with kappa distributed electrons and hot protons. The results match with Lakhina and Singh[18] (see their Eq. (14)). Further, these results also match with Singh et al.[21] for the case of $\beta = 1$, i.e., in the case of parallel propagation along the ambient magnetic field.

The third derivative of the Sagdeev pseudopotential, $S(\phi, M)$, evaluated at $\phi = 0$ is given by

$$\left(\frac{d^3S(\phi,M)}{d\phi^3}\right)_{\phi=0} = \frac{3n_{p0}\left(M^2+\sigma_p\right)}{\left(M^2-3\sigma_p\right)^3} + \frac{3n_{i0}Z_i{}^3\left(\dfrac{M^2}{\mu_{pi}}+\sigma_i\right)}{\left(\dfrac{M^2}{\mu_{pi}}-3\sigma_i\right)^3}$$

$$-\frac{(4\kappa^2-1)}{(2\kappa-3)^2}. \tag{10}$$

The positive (negative) values of Eq. (10) correspond to ion-acoustic solitons having positive (negative) electrostatic potential, ϕ. Solitons with $\phi > 0$ ($\phi < 0$) are called positive (negative) polarity solitons.

In Section III, numerical results are carried out for the slow solar wind parameters.

III. NUMERICAL RESULTS

For the parameters relevant to the solar wind plasma, the critical Mach numbers, M_0, are found from the numerical solution of Eq. (8). In general, Eq. (8) yields four roots, but all the roots are not physical. We consider only real positive roots for M_0. There are two positive roots for M_0, the smaller root corresponds to the slow ion-acoustic mode and the larger root corresponds to the fast ion-acoustic mode. The slow ion-acoustic mode is actually an ion-ion hybrid mode that requires essentially two ion species having different thermal velocities,[18] and the fast ion-acoustic mode is the usual ion-acoustic mode. The solitary solutions exist only for Mach numbers exceeding the critical Mach number ($M > M_0$).

The fast and the slow solar wind are classified on the basis of following normalized parameters. For the fast solar wind: proton to electron temperature ratio, $\sigma_p \geq 1$, heavier ion to electron density ratio, $n_{i0}/n_{e0} = 0.0 - 0.05$, and heavier ion to proton temperature ratio, $T_i/T_p \geq 1$, whereas for slow solar wind, $\sigma_p < 1$, $n_{i0}/n_{e0} = 0.0 - 0.05$, and $T_i/T_p \geq 1$. These data sets are considered on the basis of various solar wind observations.[15,18,22]

For the varied solar wind plasma parameters, we observe both fast and slow ion-acoustic modes. For the normalized parameters corresponding to the slow solar wind, $n_{i0} = 0.05$, $\sigma_p = 0.2$, $\sigma_i = 0.8$, and $\kappa = 2$, we observe only the fast ion-acoustic mode. This is in agreement with the observations of Lakhina and Singh[18] that when $T_i/T_p = 4.0$, the slow ion-acoustic mode cannot exist.

Figure 1(a) shows the variation of Sagdeev potential $S(\phi,M)$ versus the normalized electrostatic potential ϕ for various values of the Mach number for the fast ion-acoustic mode. We observe that the amplitude increases with the increase in the Mach number, till the upper limit M_{max} is reached. M_{max} is the Mach number beyond which the soliton solution ceases to exist. Here, the upper limit M_{max} on the Mach number is provided by the restriction that the lighter ion density n_p be real. This is in contrast with the observations of Lakhina and Singh[18] that the upper limit, in the case of finite relative drift velocity, for fast ion-acoustic mode is provided by the restriction that the heavier ion number density n_i should be real. Figure 1(b) shows the profiles of normalized potential ϕ with ξ. It is seen that the solitons have

symmetric profiles. Here, we observe that the soliton amplitude increases with increase in the Mach number. On the other hand, the width decreases with the increase in Mach number. The electric field profiles exhibit a similar trend as shown in Figure 1(c). It is seen that the electric field for solitons has bipolar structures.

When $T_i/T_p \neq 4.0$, we have both slow and fast ion-acoustic modes. It is found that slow ion-acoustic mode supports both positive and negative potential solitons/double layers. Also, the upper limit in the Mach number, M_{max}, in case of positive solitons in slow ion-acoustic mode is provided either by the restriction that the proton number density, n_p, be real or by the occurrence of a double layer. However, it is found that the number densities do not play any role in limiting the upper value of Mach number, M_{max}, in case of negative potential solitons. The occurrence of M_{max} in case of negative potential solitons can be attributed either to the occurrence of a double layer or to the violation of any of the conditions to be satisfied by the Sagdeev pseudopotential for soliton solution to exist.

For the normalized parameters corresponding to slow solar wind, $n_{i0} = 0.05$, $\sigma_p = 0.2$, $\sigma_i = 1.1$, and $\kappa = 2$, we observe that the slow ion-acoustic mode supports a negative double layer. Figure 2(a) shows the variation of Sagdeev potential $S(\phi,M)$ versus the normalized electrostatic potential ϕ for various values of the Mach number. Here, the amplitude increases with the increase in the Mach number, until the maximum Mach number, M_{max}, is reached. Here, the upper limit on the occurrence of the soliton is provided by the appearance of a double layer at $M = 0.9005865$. The double layer profile has been marked as DL in the figure for clarity. Figure 2(b) shows the profiles of normalized potential ϕ with ξ. It is seen that the double layers have asymmetric profiles. Here, we observe that the soliton amplitude as well as the width increases with increase in the Mach number. Dombeck *et al.*[23] have observed from the data of POLAR satellite a similar trend of increase in the width with increasing amplitude in the auroral region. Later on, Ghosh and Lakhina[7] studied the anomalous width-amplitude variation using a plasma model consisting of two electrons species with different temperatures. They called the behaviour anomalous as soliton width increased with the increase in amplitude which was different than the generally observed for K-dV (small amplitude) solitons where width was found to decrease with increase in amplitude. The electric field profiles exhibit a similar trend as shown in Figure 2(c). It is seen that the electric field for double layers has monopolar structures (marked as DL).

For the normalized parameters corresponding to slow solar wind, $n_{i0} = 0.05$, $\sigma_p = 0.2$, $\sigma_i = 1.3$, and $\kappa = 2$, slow ion-acoustic mode is found to support a positive double layer. Figure 3(a) shows the variation of Sagdeev pseudopotential $S(\phi,M)$ versus the normalized electrostatic potential ϕ. A trend similar in characteristic to Figure 2(a) is observed. The plot of normalized potential, ϕ versus ξ, and normalized electric field, E versus ξ, is shown in Figures 3(b) and 3(c), respectively. Here, the amplitude of the solitons increases with the Mach number. However, the width of the soliton is

(a)

(b)

(c)
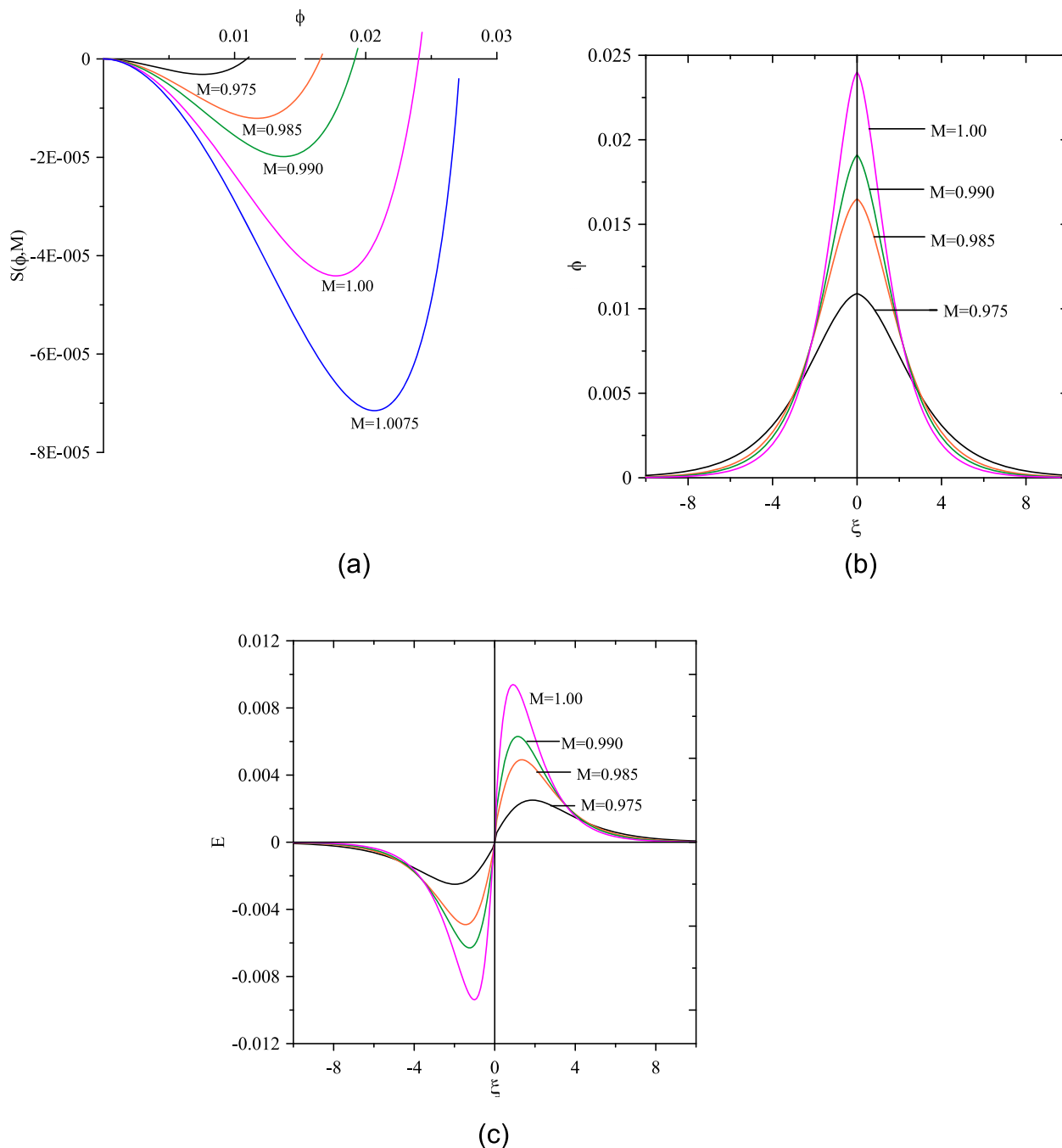
FIG. 1. Fast ion-acoustic mode: Panel (a) shows plot of Sagdeev pseudopotential $S(\phi, M)$ vs the normalized potential ϕ. Panel (b) shows plot of normalized potential ϕ vs ξ. Panel (c) shows plot of the normalized electric field E varying with ξ. The normalized parameters considered are: $n_{i0} = 0.05$, $\sigma_p = 0.2$, $\sigma_i = 0.8$, and $\kappa = 2$.

found to decrease as the Mach number increases. The electric field profiles follow the same trend as in Figure 2(c).

Figure 4 shows the variation of critical Mach number, M_0, maximum Mach number, M_{max}, and maximum value of the potential, ϕ_{max}, with n_{i0} for the parameters relevant to slow solar wind $\sigma_p = 0.2$, $\sigma_i = 0.4$, and $\kappa = 2$. M_{max} corresponds to the maximum Mach number at which the soliton solution ceases to exist. The electric potential amplitude ϕ corresponding to M_{max} is designated as ϕ_{max}. Plot (a) shows the variation for slow ion-acoustic mode, while plot (b) shows the variation for fast ion-acoustic mode. We observe that M_0, M_{max}, and ϕ_{max} increase with the increase in n_{i0} for

slow ion-acoustic mode, whereas they decrease with the increase in n_{i0} for fast ion-acoustic mode.

Figure 5 shows the variation of critical Mach number, M_0, maximum Mach number, M_{max}, and maximum value of the potential, ϕ_{max}, with κ for the same parameters corresponding to Figure 4 with $n_{i0} = 0.05$. Plot (a) shows the variation for slow ion-acoustic mode, while plot (b) shows the variation for fast ion-acoustic mode. We observe that M_0, M_{max}, and ϕ_{max} gradually increase with the increase in κ for both slow and fast ion-acoustic modes. However, the existence domain for solitons is greater in fast ion-acoustic mode as compared to slow ion-acoustic mode. For fast ion acoustic
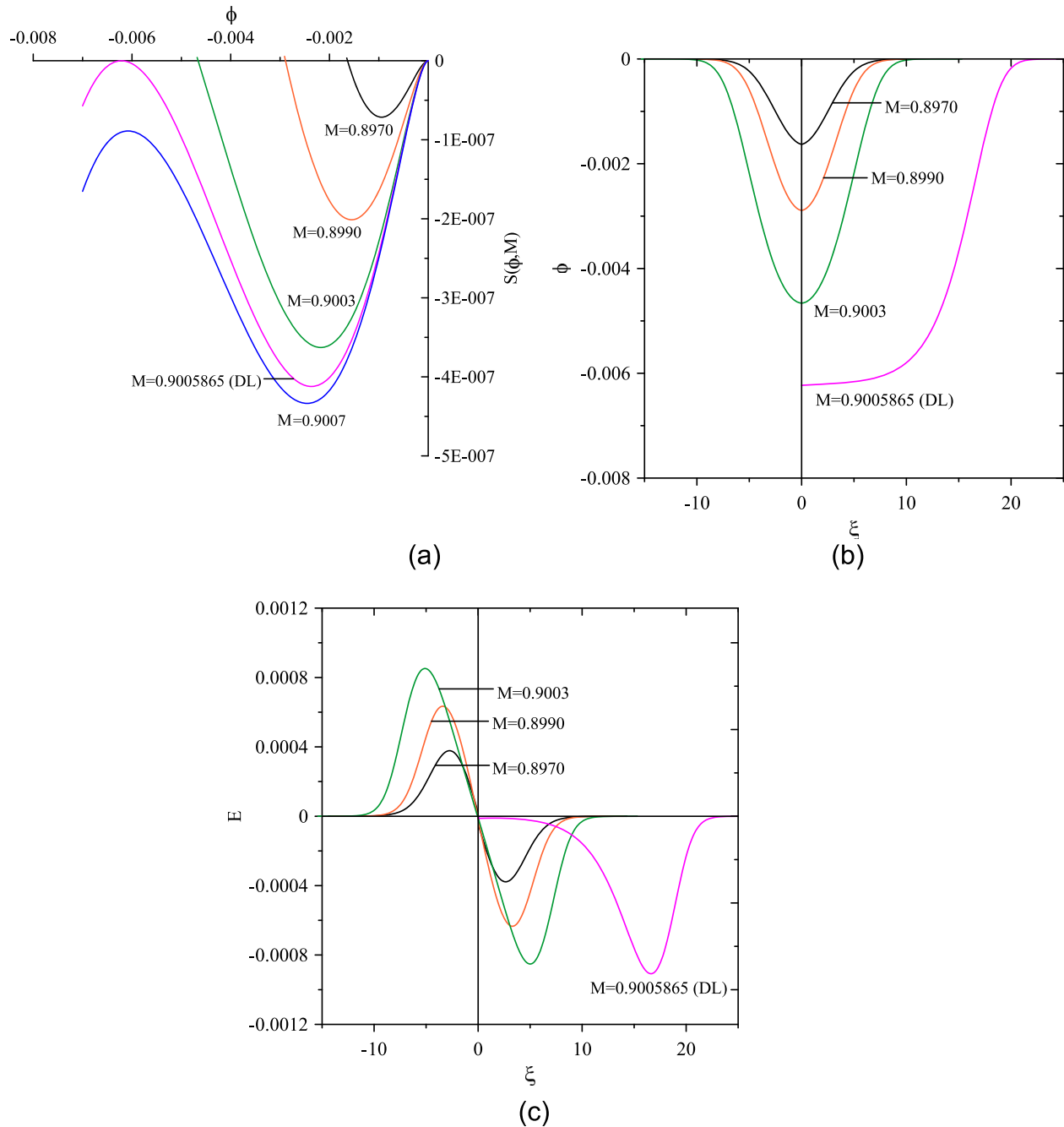
FIG. 2. Slow ion-acoustic mode: Panel (a) shows plot of Sagdeev pseudopotential $S(\phi, M)$ vs the normalized potential ϕ. Panel (b) shows plot of normalized potential ϕ vs ξ. Panel (c) shows plot of the normalized electric field E varying with ξ. The normalized parameters considered are: $n_{i0} = 0.05$, $\sigma_p = 0.2$, $\sigma_i = 1.1$, and $\kappa = 2$.

mode, we have $0.0469 \leq M_{max} - M_0 \leq 0.116$, while slow ion acoustic mode varies as $0.0023 \leq M_{max} - M_0 \leq 0.0033$.

Figure 6 shows the existence curve for the slow ion-acoustic solitons/double layers with respect to σ_i for the parameters relevant to the slow solar wind. The normalized parameters considered here are: $n_{i0} = 0.05$, $\sigma_p = 0.2$, and $\kappa = 2$. The existence domains of solitons and double layers are clearly demarcated with dashed vertical lines. Panel (a) shows the variation of $M_{max} - M_0$ with σ_i. We find that, for $\sigma_i < 0.8$, i.e., $T_i < 4T_p$ (region-I), we only have positive potential solitons. Furthermore, we observe that, as reported by Lakhina and Singh[18] when $T_i = 4T_p$, i.e., at $\sigma_i = 0.8$, the

slow ion-acoustic mode ceases to exist. Hence, we have a gap at $\sigma_i = 0.8$ in the existence curve. In region-II, $0.8 < \sigma_i \leq 1.0$, we observe negative potential solitons, followed by negative double layers in region-III, $1.0 < \sigma_i < 1.24$. Transition from negative soliton/double layers to the positive soliton/double layers takes place at $\sigma_i = 1.24$. In the region-IV, the positive double layers are observed for $1.24 \leq \sigma_i \leq 1.4$. The variation of corresponding maximum potential, ϕ_{max}, with σ_i is shown in panel (b). The empty circles (region-III) and + sign (region-IV) on the curve show the existence of negative and positive double layers, respectively. For further increase in the ion

(a)

(b)

(c)
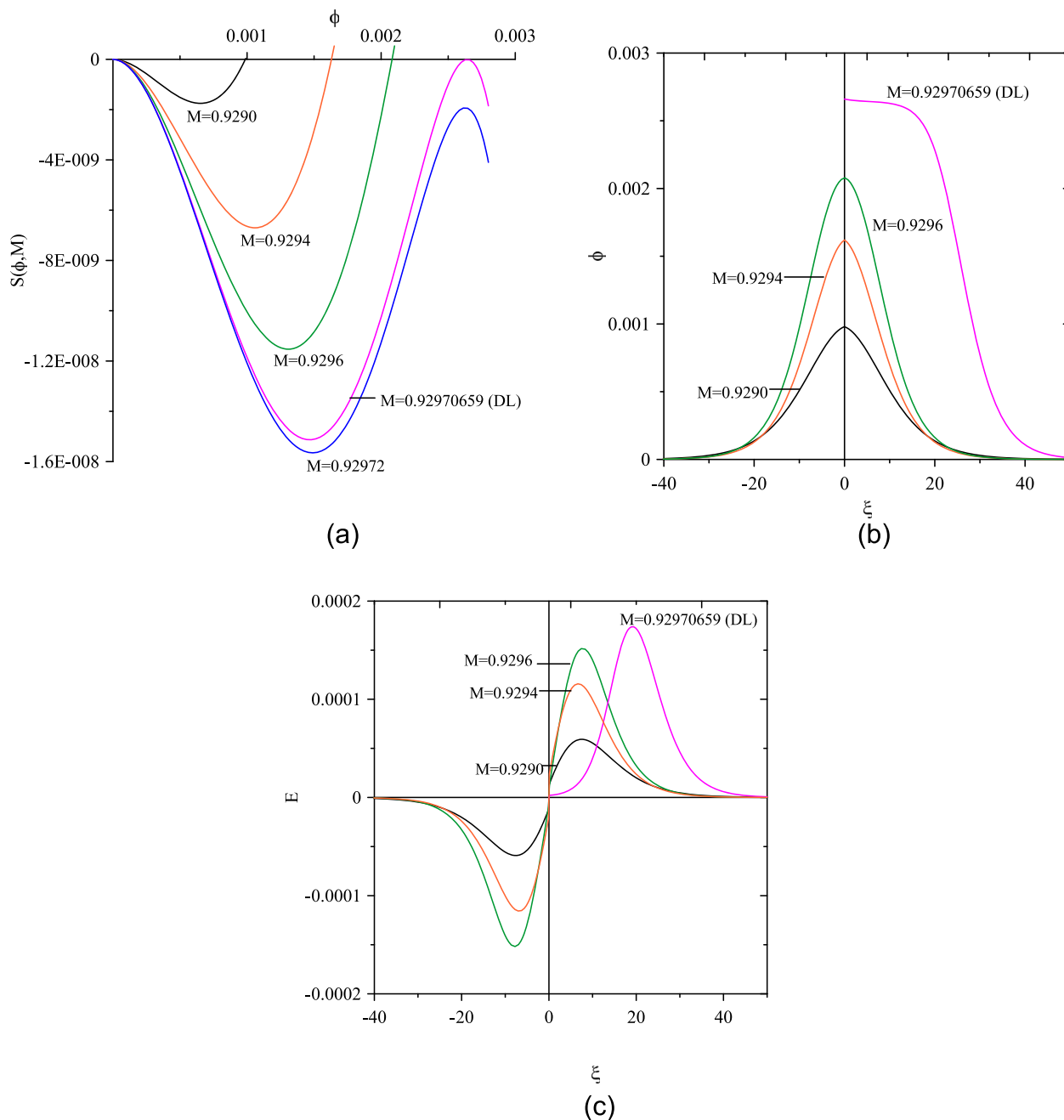
FIG. 3. Slow ion-acoustic mode: Panel (a) shows plot of Sagdeev pseudopotential $S(\phi, M)$ vs the normalized potential ϕ. Panel (b) shows plot of normalized potential ϕ vs ξ. Panel (c) shows plot of the normalized electric field E varying with ξ. The normalized parameters considered are: $n_{i0} = 0.05$, $\sigma_p = 0.2$, $\sigma_i = 1.3$, and $\kappa = 2$.

temperature, i.e., for $\sigma_i > 1.4$, positive potential solitons are observed as shown in region-V.

The switch in the polarity of the slow ion-acoustic solitons is consistent with the change in the polarity of the third derivative of $S(\phi, M)$ evaluated at $\phi = 0$ (Eq. (10)) and $M = M_0$.[11,24] For the parameters of Figure 6, in regions $\sigma_i < 0.8$ and $\sigma_i \geq 1.24$, we find that $\left(\frac{d^3 S(\phi, M)}{d\phi^3} \right)_{\phi=0} > 0$, signifying positive polarity solitons, while in regions $0.8 < \sigma_i < 1.24$, we have $\left(\frac{d^3 S(\phi, M)}{d\phi^3} \right)_{\phi=0} < 0$, signifying negative polarity solitons.

From Figure 6, it is clear that $M_{max} - M_0$ as well ϕ_{max} decreases with σ_i in region-I ($\sigma_i < 0.8$). This signifies that

the region over which soliton profile exists decreases as the temperature of the ion (T_i) increases, till $T_i = 4T_p$. In region-II, the range ($M_{max} - M_0$) increases with σ_i, followed by a decrease in region-III, and thereafter, in the regions-IV and V, $M_{max} - M_0$ increases with increasing σ_i. The maximum electric potential amplitude, ϕ_{max}, becomes negative in regions II and III. ϕ_{max} decreases in region-II. In the region-III, ϕ_{max} decreases initially and then shows a gradual increase. The polarity of ϕ_{max} changes from region-III to IV, showing a transition from negative solitons/double layers to positive solitons/double layers. The maximum potential, ϕ_{max}, tends to increase till it almost becomes constant in region-V beyond $\sigma_i \approx 1.8$.
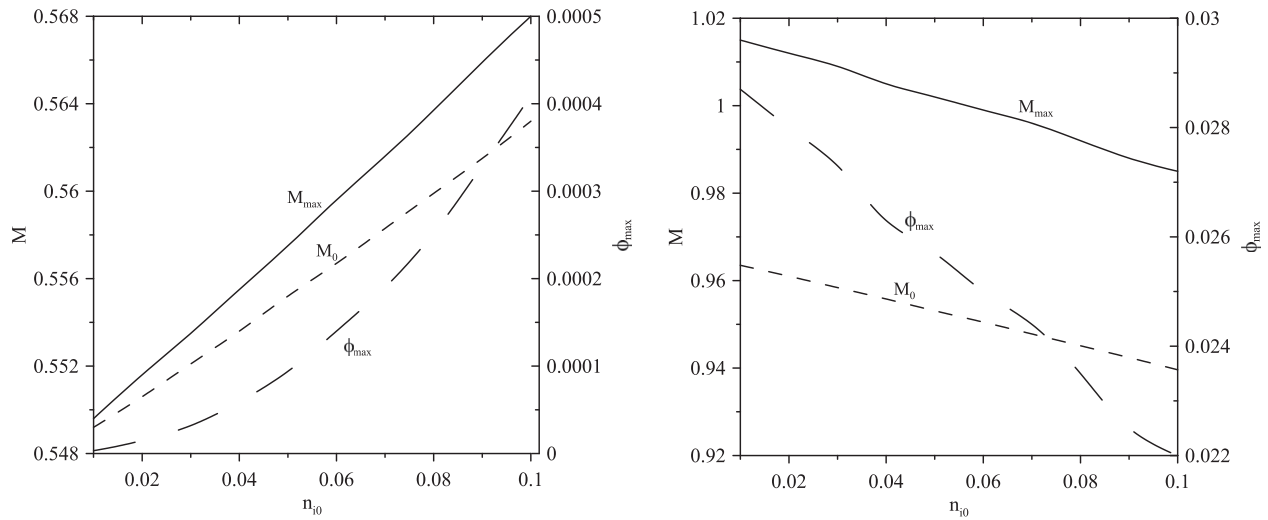
FIG. 4. Variation of critical Mach number, M_0 (dashed curves), maximum Mach number, M_{max} (solid curves), and maximum value of the potential, ϕ_{max}(long-dashed curve), with n_{i0} for (a) slow ion-acoustic mode and (b) fast ion-acoustic mode. The normalized parameters are $\sigma_p = 0.2$, $\sigma_i = 0.4$, and $\kappa = 2$. Here, the Y-axis on the left hand side (L.H.S) shows the scale for Mach number, while on the right hand side (R.H.S) shows the scale for maximum electric potential amplitude ϕ_{max}.

Figure 7 shows the variation of $M_{max} - M_0$ and ϕ_{max} with σ_i for fast ion-acoustic mode with the same parameters as in Figure 6. We observe that both $M_{max} - M_0$ and ϕ_{max} show almost similar trend. Initially, both increase gradually as σ_i increases and then show a sudden decrease around $\sigma_i = 0.7$. Thereafter, around $\sigma_i = 1.6$, both become constant.

IV. DISCUSSION AND CONCLUSIONS

Electrostatic solitary waves in a magnetized three component plasma consisting of hot heavier ions (alpha particles), hot protons, and suprathermal electrons have been examined. The existence domains for slow and fast ion-acoustic solitons/double layers are analyzed over varied parametric regimes relevant to the solar wind.

It is found that for a large number of parameters relevant to the slow solar wind both fast and slow ion-acoustic solitons/double layers exist. However, when $T_i = 4T_p$, the slow ion-acoustic solitons cease to exist. The fast ion-acoustic solitons are found to be similar to the usual ion-acoustic solitons (solitons found in electron-proton plasmas). The slow ion-acoustic mode is a new ion-ion hybrid mode, which essentially owes its existence to the difference in thermal velocities between the two ions (here, protons and alpha particles). The fast ion-acoustic mode supports only positive potential solitons. The slow ion-acoustic mode supports both positive potential solitons/double layers and negative potential solitons/double layers. The earlier studies on existence domains of electron/ion-acoustic solitons/double layers have shown transition occurring due to the change in cool electron
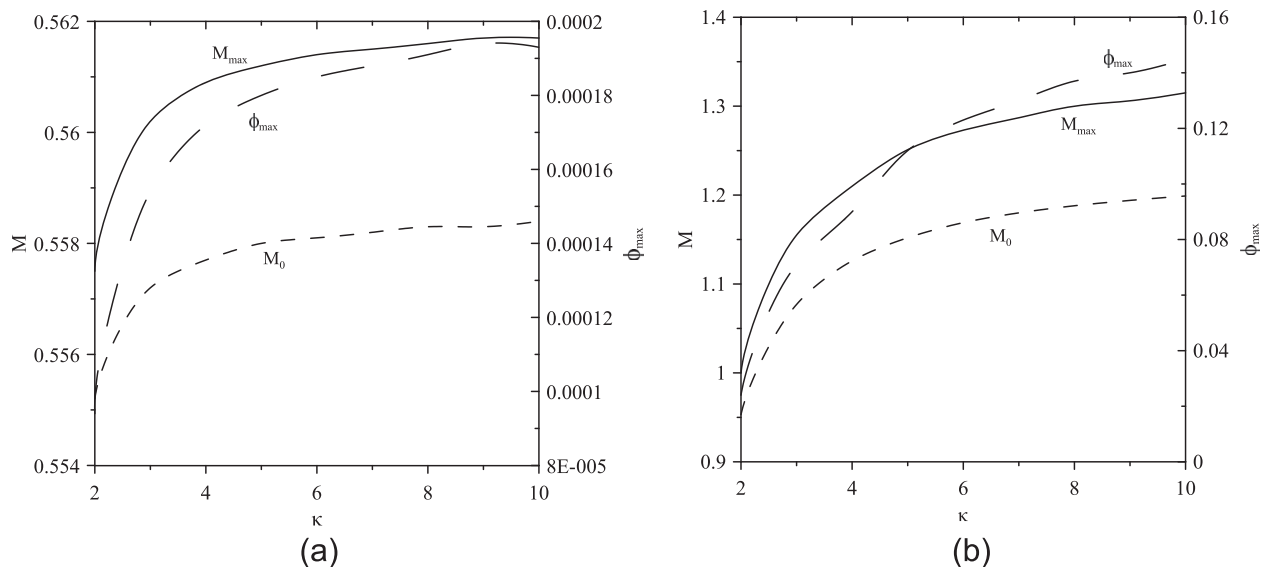
FIG. 5. Variation of critical Mach number, M_0 (dashed curves), maximum Mach number, M_{max} (solid curves), and maximum value of the potential, ϕ_{max} (long-dashed curve), with κ for (a) slow ion-acoustic mode and (b) fast ion-acoustic mode. The normalized parameters are $n_{i0} = 0.05$, $\sigma_p = 0.2$, and $\sigma_i = 0.4$. Here, the Y-axis on the left hand side (L.H.S) shows the scale for Mach number, while on the right hand side (R.H.S) shows the scale for maximum electric potential amplitude ϕ_{max}.
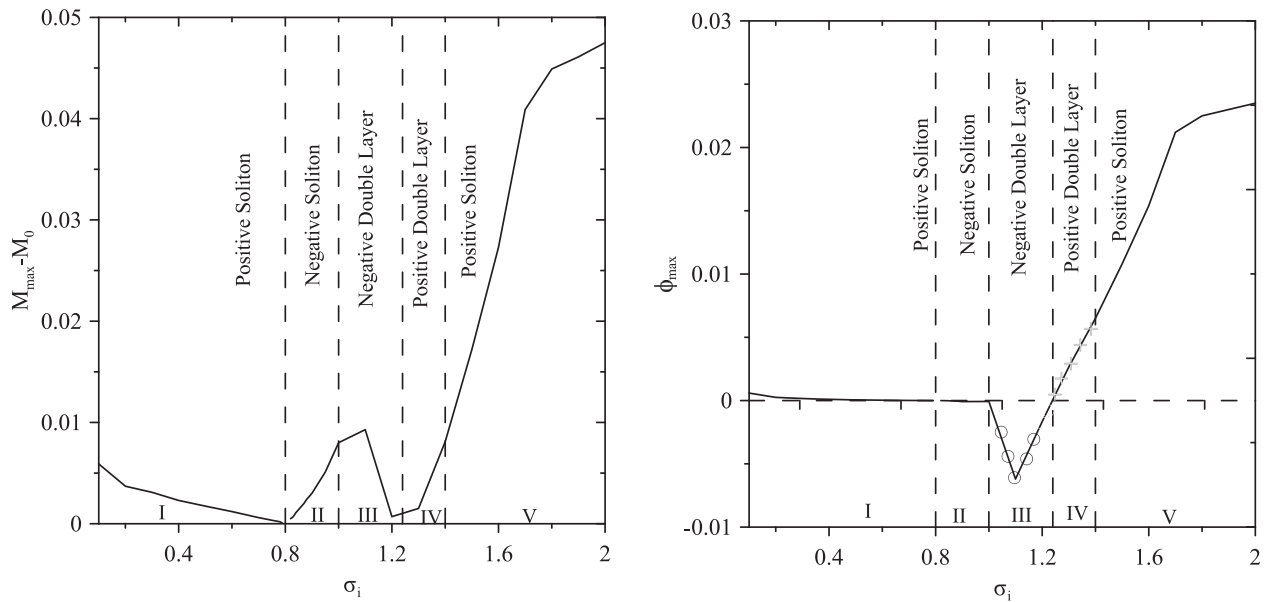
FIG. 6. Existence domains of slow ion-acoustic soliton are depicted as a function of σ_i for the normalized parameters $n_{i0} = 0.05$, $\sigma_p = 0.2$, and $\kappa = 2$. Positive solitons exist in region-I and V, while negative solitons occur in region-II. Marks of circles (region-III) and $+$ sign (region-IV) on ϕ_{max} show the existence of negative and positive double layers, respectively. At $\sigma_i = 0.8$, the slow ion-acoustic mode ceases to exist and we observe a gap in the $M_{max} - M_0$ curve as well as in the ϕ_{max} curve.

density.[9–11] Here, for the first time, a transition from negative potential soliton/double layers to positive potential soliton/double layers with respect to temperature of the ions (alpha particles) is observed for slow ion-acoustic solitons.

It is also observed that the velocity of slow ion-acoustic mode is greater than the thermal velocity of protons (V_{tp}), but is lesser than the thermal velocity of heavier ions (V_{ti}), while the velocity of fast ion-acoustic solitons is greater than the thermal velocity of heavier ions (V_{ti}), but is lesser than the thermal velocity of the suprathermal electrons (V_{te}): $\sqrt{3}V_{tp} < V_{slow} < \sqrt{3}V_{ti} < V_{fast} < \sqrt{3}V_{te}$.
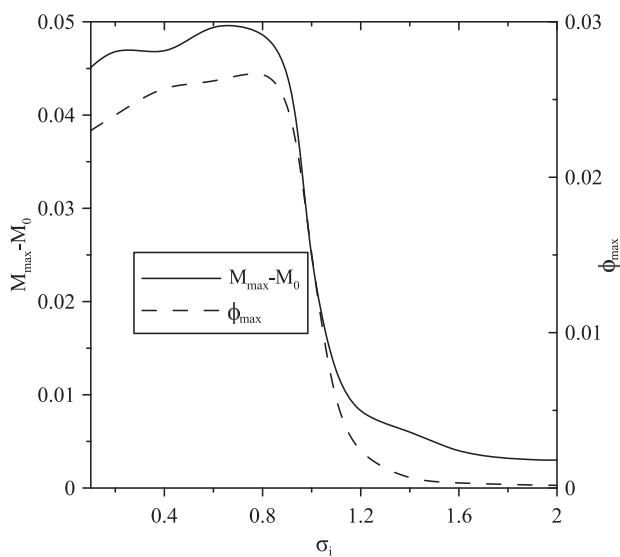
FIG. 7. Existence domains of fast ion-acoustic soliton are depicted as a function of σ_i for the normalized parameters $n_{i0} = 0.05$, $\sigma_p = 0.2$, and $\kappa = 2$. Here, the Y-axis on the left hand side (L.H.S) shows the scale for Mach number $(M_{max} - M_0)$, while on the right hand side (R.H.S) shows the scale for maximum electric potential amplitude ϕ_{max}.

In both the fast and slow ion-acoustic modes, the amplitude of the soliton increases with the increase in the Mach number till the upper limit on Mach value is reached. For fast ion-acoustic solitons, the width is found to decrease with the increase in the Mach number. However, for the slow ion-acoustic mode, the width of the solitons increases with the increase in the Mach number for negative potential solitons. The width variation trend is similar to the observed trend of rarefactive ion-acoustic solitons in the auroral plasma by the POLAR satellite,[23] while in case of positive potential solitons, width is found to decrease with the Mach number, similar to the fast ion-acoustic mode. The limitation on the attainable amplitudes of solitons in fast ion-acoustic mode is attributed to that the number density of lighter ion n_p should remain real till the upper Mach number limit is reached, while for the slow ion-acoustic mode, for the positive potential solitons, the upper limit on amplitude is provided either by the requirement that the heavier ion number density n_i should be real or by the existence of the positive double layer. The negative potential soliton is found to be limited by either the violation of the condition to be satisfied by Sagdeev pseudopotential for the soliton profile to exist or by the existence of negative potential double layer.

For different parametric regimes, we observe that for fast ion-acoustic mode, M_0, M_{max}, and ϕ_{max} decrease with the increase in the n_{i0}. The difference between M_{max} and M_0 almost remains constant with increasing n_{i0}. In the case of slow ion-acoustic mode, M_0, M_{max}, and ϕ_{max} increase with the increase in the n_{i0}. However, in this case too, the difference between M_0 and M_{max} almost remains constant with increasing n_{i0}.

M_0, M_{max}, and ϕ_{max} increase gradually with the increase in the suprathermality index, κ, for both the slow and fast ion acoustic modes. However, the difference between M_0

TABLE I. Properties of fast and slow ion-acoustic solitons for various values of σ_i for the normalized parameters, $n_{i0} = 0.05$, $\sigma_p = 0.2$, and $\kappa = 2$. Here, temperature of electron, $T_e = 10$ eV, and total number density of electrons, $n_0 = 7.75$ cm^{-3}, are used for numerical estimation of the relevant properties.

σ_i	V (km s^{-1})	E (peak-to-peak) (mV m^{-1})	W (m)	Polarity of the solitons
0.8 (Slow)	…	Does not exist	…	
1.1 (Slow)	27.64–27.92	0.007–2.15	160–222	−ve
1.3 (Slow)	28.78–28.82	0.005–0.42	290–530	+ve
0.8 (Fast)	29.68–31.19	0.002–27.4	23–794	+ve
1.1 (Fast)	30.18–30.53	0.007–2.91	45–430	+ve
1.3 (Fast)	31.49–31.68	0.04–0.68	40–120	+ve

and M_{max} is larger for the fast ion-acoustic mode as compared to the slow ion-acoustic mode.

It is found that the slow ion-acoustic mode supports only positive potential solitons for $\sigma_i < 0.8$. As σ_i is increased, it supports negative potential solitons/double layers. For further increase in σ_i, there is a transition from negative potential double layers to positive potential double layers. For still higher values of σ_i, the slow ion-acoustic mode is found to support only positive potential solitons.

We apply our theoretical model to explain the observations of the electrostatic waves by the time domain sampler (TDS) on WIND. For numerical estimation of the physical properties of the electrostatic waves, we have used the parameters:[15,18] temperature of electron, $T_e = 10$ eV and total number density of electrons, $n_0 = 7.75$ cm^{-3}. For these parameters, the ion-acoustic speed, $C_a = 31$ km/s, and the effective hot electron Debye length, $\lambda_{de} = 844$ cm.

In Table I, the unnormalized soliton velocity (V), electric field (E), and soliton width (W) for various σ_i values are given for the fast and slow ion-acoustic modes. Here, the width, W, is defined as the full width at half maximum.

We observe from the Table I that for $\sigma_i = 0.8$, only fast ion-acoustic mode exists which is in confirmation with the analytical expression given by Eq. (8), since at $T_i = 4T_p$, we get only one physical root from Eq. (8) which corresponds to the fast ion-acoustic mode. It is seen that the velocity of the solitons increases with σ_i for both slow and fast ion-acoustic modes. However, the peak-to-peak electric field is found to decrease with increasing values of σ_i. Here, the velocity and the electric field of the fast ion-acoustic solitons are greater than the slow ion-acoustic solitons. The width range increases for increasing values of σ_i for both negative and positive polarity slow ion-acoustic solitons. However, the width range decreases with σ_i for fast ion acoustic solitons. In Table I, for the positive polarity solitons (both slow and fast), the higher values of the width correspond to the lower soliton velocity. However, for negative polarity slow ion-acoustic solitons, the higher value of width corresponds to the higher velocity. Malaspina et al.[16] reported that the peak-to-peak electric field amplitude of the electrostatic solitary waves in the solar wind observed by the TDS onboard the WIND range from $(0.1 - 8)$ mV/m with an average of 0.5 mV/m. From Table I, we find that the calculated peak-to-peak electric field amplitude for both slow and fast ion-acoustic modes

matches with the observed low-frequency waves in the solar wind at $\sigma_i = 1.1$ and 1.3. For the remaining values of the σ_i, we find that corresponding to the lower velocity values, the peak-to-peak electric field amplitude agrees with the observed amplitudes.

It is important to point out that the theoretical model presented here deals with the time stationary state of the plasma system when the plasma instabilities, if present initially, have been saturated. In a sense, the model deals with the nonlinear modes of the system. The homogeneous plasma model can be applicable to observations[16] as long as the magnetic discontinuity scale lengths are larger than the widths of solitary structures, for both solitons and the double layers.

ACKNOWLEDGMENTS

[1]H. Washimi and T. Taniuti, Phys. Rev. Lett. **17**, 996 (1966).
[2]W. D. Jones, A. Lee, S. M. Gleman, and H. J. Doucett, Phys. Rev. Lett. **35**, 1349 (1975).
[3]B. N. Goswami and B. Buti, Phys. Lett. A **57**, 149–150 (1976).
[4]S. Baboolal, R. Bharuthram, and M. A. Hellberg, J. Plasma Phys. **44**, 1–23 (1990).
[5]R. A. Cairns, A. A. Mamun, R. Bingham, and P. K. Shukla, Phys. Scr. **1996**, 80.
[6]M. Berthomier, R. Pottelette, and M. Malingre, J. Geophys. Res. **103**, 4261, doi:10.1029/97JA00338 (1998).
[7]S. S. Ghosh and G. S. Lakhina, Nonlinear Process. Geophys. **11**, 219 (2004).
[8]S. V. Singh, G. S. Lakhina, R. Bharuthram, and S. R. Pillay, Phys. Plasmas **18**, 122306 (2011).
[9]G. S. Lakhina, A. P. Kakad, S. V. Singh, and F. Verheest, Phys. Plasmas **15**, 062903 (2008).
[10]G. S. Lakhina, A. P. Kakad, S. V. Singh, F. Verheest, and R. Bharuthram, Nonlinear Process. Geophys. **15**, 903 (2008).
[11]S. K. Maharaj, R. Bharuthram, S. V. Singh, and G. S. Lakhina, Phys. Plasmas **19**, 072320 (2012).
[12]S. K. Maharaj, R. Bharuthram, S. V. Singh, and G. S. Lakhina, Phys. Plasmas **22**, 032313 (2015).
[13]D. A. Gurnett and R. R. Anderson, J. Geophys. Res. **82**(4), 632–650, doi:10.1029/JA082i004p00632 (1977).
[14]D. A. Gurnett and L. A. Frank, J. Geophys. Res. **83**, 58–74, doi:10.1029/JA083iA01p00058 (1978).
[15]A. Mangeney, C. Salem, J. C. Lacombe, C. Perche, R. Manning, P. J. Kellogg, K. Geoz, S. J. Monson, and J. M. Bosqued, Ann. Geophys. **17**, 307–320 (1999).
[16]D. M. Malaspina, D. L. Newman, L. B. Willson, K. Goetz, P. J. Kellogg, and K. Kerstin, J. Geophys. Res. - Space Phys. **118**, 591–599, doi:10.1002/jgra.50102 (2013).
[17]G. S. Lakhina, S. V. Singh, and A. P. Kakad, Phys. Plasmas **21**, 062311 (2014).
[18]G. S. Lakhina and S. V. Singh, Sol. Phys. **290**, 3033–3049 (2015).
[19]R. M. Thorne and D. Summers, Phys. Fluids B **3**, 2117 (1991).
[20]S. Devanandhan, S. V. Singh, and G. S. Lakhina, Phys. Scr. **84**, 025507 (2011).
[21]S. V. Singh, S. Devanandhan, G. S. Lakhina, and R. Bharuthram, Phys. Plasmas **20**, 012306 (2013).
[22]J. E. Borovsky and S. P. Gary, J. Geophys. Res. - Space Phys. **119**, 5210–5219, doi:10.1002/2014JA019758 (2014).
[23]J. Dombeck, C. Cattell, and J. Crumley, J. Geophys. Res. **106**, 19013–19021, doi:10.1029/2000JA000355 (2001).
[24]S. K. Maharaj, R. Bharuthram, S. V. Singh, and G. S. Lakhina, Phys. Plasmas **19**, 122301 (2012).